Three-dimensional labyrinthine acoustic metamaterials

Tobias Frenzel, Jan David Brehm, Tiemo Bückmann, Robert Schittny, Muamer Kadic et al.

Additional information on Appl. Phys. Lett.

Three-dimensional labyrinthine acoustic metamaterials

Tobias Frenzel,[1,a)] Jan David Brehm,[1,a)] Tiemo Bückmann,[1] Robert Schittny,[1,b)] Muamer Kadic,[1] and Martin Wegener[1,2]

[1]*Institute of Applied Physics, Karlsruhe Institute of Technology (KIT), 76128 Karlsruhe, Germany*
[2]*Institute of Nanotechnology, Karlsruhe Institute of Technology (KIT), 76128 Karlsruhe, Germany*

Building upon recent theoretical and experimental work on two-dimensional labyrinthine acoustic metamaterials, we design, fabricate, and characterize nearly isotropic three-dimensional airborne acoustic labyrinthine metamaterials. Our experiments on aluminum-based structures show phase and group velocities smaller than that of air by a factor of about 8 over a broad range of frequencies from 1 to 4 kHz. This behavior is in agreement with three-dimensional band-structure calculations including the first and higher bands. The extracted imaginary parts of the phase velocity are 5–25 times smaller than the mentioned real parts. This ratio is better than for most optical metamaterials but still rather favors applications in terms of sub-wavelength broadband acoustic absorbers. © 2013 AIP Publishing LLC. [http://dx.doi.org/10.1063/1.4817934]

Recently, labyrinthine or "space coiling" metamaterials were theoretically suggested for airborne acoustics.[1] The labyrinth motif complements other possibilities for broadband slowing-down of acoustic waves, e.g., by using rod-based sonic crystals in the long-wavelength limit.[2] In essence, the underlying idea[1] is that the labyrinth provides an internal geometrical "detour" for the sound wave, which, when seen from the outside, appears as an effectively slower metamaterial phase velocity. The factor by which the detour elongates the geometrical path length can be interpreted as an effective phase refractive index. For frequencies below the first-order Bragg resonance condition, negligible effective dispersion is expected and, hence, phase and group velocity of sound are frequency-independent and identical. More recently, labyrinthine metamaterials have been fabricated and characterized experimentally in quasi-two-dimensional form for acoustics at kHz frequencies[3,4] and for electromagnetism at GHz frequencies.[3]

In this letter, we design corresponding three-dimensional labyrinthine acoustic metamaterials, calculate their band structure, fabricate them on aluminum basis with centimeter-scale lattice constants, and characterize their properties by performing pulse-propagation experiments with carrier frequencies in the kHz range. We show unprocessed experimental raw data. We also critically discuss the sign of the velocities in bands higher than the first one and give a quantitative assessment of the effective losses.

Figure 1(a) illustrates our three-dimensional generalization of the previous two-dimensional labyrinthine metamaterials. In a first layer, the structure is qualitatively similar (but not identical) to the two-dimensional case.[1] Next, the acoustic wave is guided along the vertical direction into a second layer, etc. Note that the layers are not identical and that the channels meet in the center of the depicted extended cubic unit cell. This design is made such that the geometrical path length in each of the three Cartesian directions is expanded by the same

factor of six and such that the entire volume (apart from the thin walls) is accessible to wave propagation. The resulting crystal can be thought of as arising from a body-centered-cubic (bcc) translational lattice and the primitive motif or basis depicted in panel (c) of Fig. 1. This motif breaks cubic symmetry and we will need to check whether the acoustic wave properties of the first band remain isotropic.

Corresponding band-structure calculations are shown in Fig. 2. These results are obtained from numerical solutions of the eigenvalue problem of (longitudinally polarized) pressure waves in air with hard-wall boundaries as defined in Fig. 1. This appears justified because the acoustic impedance of aluminum, which is to be used in the below experiments, is about 4×10^4 times larger than that of air under ambient conditions. This means that 99.990% of the sound energy is reflected at the air-aluminum interface. We impose periodic boundary conditions corresponding to the underlying translational lattice. We use the commercial software package COMSOL Multiphysics and neglect any type of damping at this point. The horizontal axis in Fig. 2(a) is the usual tour through the face-centered cubic (fcc) first Brillouin zone. The vertical axis on the left shows the frequency in units of Hz for a lattice constant of $a = 2.4$ cm, the vertical scale on the right the normalized frequency a/λ, where λ is the air wavelength referring to a standard-air speed of sound $c_0 = 343$ m/s. As expected from our heuristic reasoning, the phase velocity of sound derived from the slope of the first band is smaller by a factor of 7.9 than that of standard air. Note that the phase velocities for propagation along the ΓH direction (i.e., along x) and the ΓH' direction (i.e., along z) are the same. To further investigate any direction dependence, panel (b) of Fig. 2 shows selected iso-frequency contours in various planes for frequencies within the first band as indicated by the false-color scale. Obviously, the contours are nearly circular in the vicinity of the Γ point, such that we can indeed think of the labyrinthine metamaterial as an isotropic three-dimensional effective material.

In our experiments, we have fabricated a crystal out of the unit cell shown in Fig. 1 by computer-aided automated machining of aluminum in several layers (see Fig. 3). In two

a)T. Frenzel and J. D. Brehm contributed equally to this work.
b)Electronic mail: robert.schittny@kit.edu
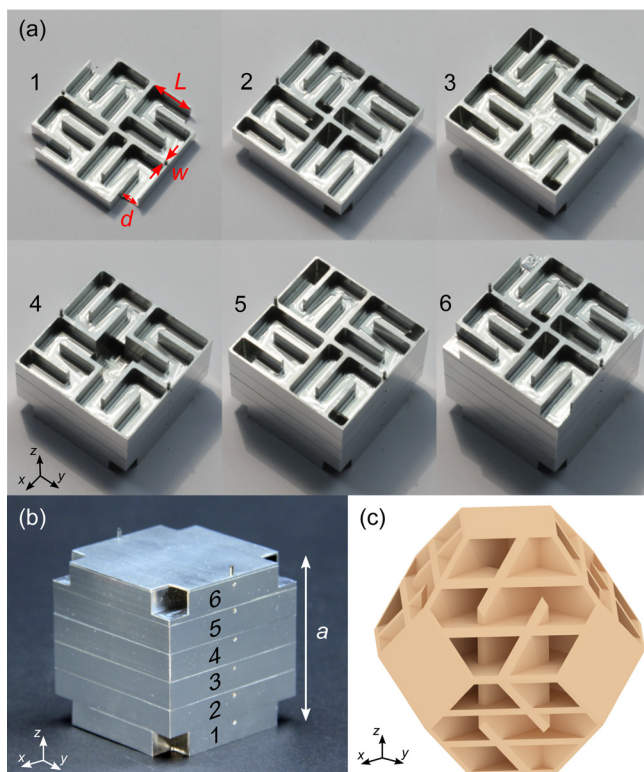
103, 061907-1

FIG. 1. (a) Photographs of the six different layers of one three-dimensional labyrinthine metamaterial extended unit cell (compare panel (b)). Note the holes connecting adjacent layers. Parameters as used in the below experiments are: lattice constant $a = 2.4$ cm, channel width $d = 0.32$ cm, wall width $w = 0.08$ cm, and wall length $L = 0.8$ cm. (b) Photograph of one assembled extended unit cell machined out of aluminum. (c) Illustration of the Wigner-Seitz (primitive) unit cell of the body-centered-cubic (bcc) lattice.
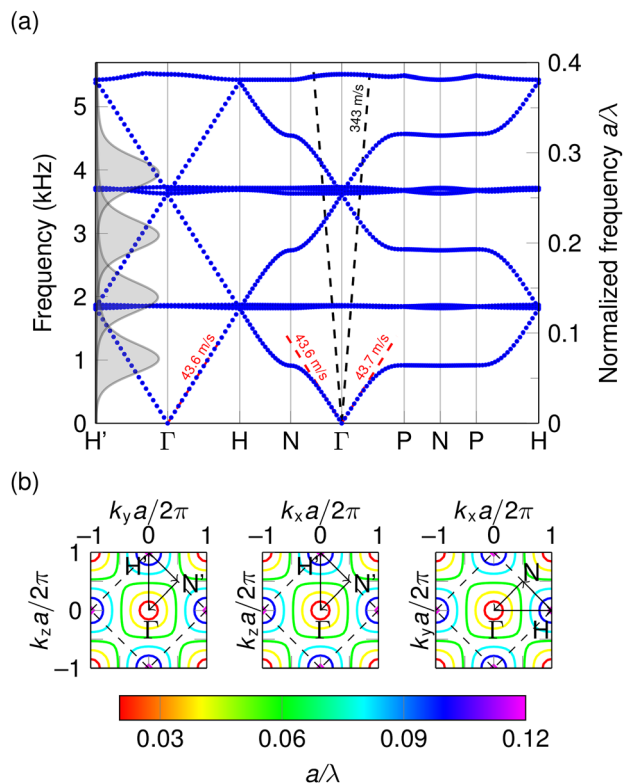

FIG. 2. (a) Calculated band structure of the acoustic labyrinthine metamaterial illustrated in Fig. 1. Phase velocities of the first band are indicated around the Γ point. On the left-hand side, power spectra of the Gaussian pulses used in the measurements are shown for four different center frequencies (see Fig. 4). There, propagation is along the z axis, equivalent to the $\Gamma H'$ direction. (b) Selected iso-frequency contours (yz-, xz-, and xy-plane in reciprocal space from left to right) showing isotropic behavior for the first band around the Γ point. The border of the first Brillouin zone is indicated by the dashed straight lines.

of the three orthogonal main cubic directions (x and y), the number of lattice constants is fixed and equal to 5. In the orthogonal z direction, which is the propagation direction in the experiments, we can flexibly and reversibly choose the number of lattice constants N. $N = 1, 2, 3, 4, 5$ are possible with the fabricated set of layers. Airborne acoustic waves are launched by a loudspeaker in a distance of about one meter from the sample and detected by a sensitive capacitive microphone (beyerdynamic MM1) in a distance of about 20 cm from the sample on the other side. As usual, the microphone signal is proportional to the local wave-pressure variation. Both loudspeaker and microphone are connected to a personal computer, allowing for controlling the carrier and the envelope of the launched pulses as well as for data averaging. We choose sin-pulses, i.e., pulses for which the carrier wave has a zero crossing at the peak of the envelope. Their power spectrum has strictly zero amplitude at zero frequency. In contrast, few-cycle cos-pulses do have a finite zero-frequency amplitude, which can give rise to artifacts because the zero-frequency component gets lost during propagation. We fix the absolute duration of the envelope, i.e., the ratio of duration to sound period changes when varying the center frequency. In this fashion, the power spectra at different carrier frequencies have a fixed spectral width (see Fig. 2). The sample is placed in the opening of a big box (a small room in a room) which is acoustically isolated from its outside and damped from the inside using absorbing foam

plates, aiming at preventing partial waves to propagate around the sample. During the experiments, the temperature in the room was constant to within $\pm 1\,^\circ$C, which translates into a relative change of the air speed of sound of $\pm 0.2\,\%$. In what follows, we show unprocessed raw data rather than only retrieved effective metamaterial parameters.

Fig. 4 exhibits the measured microphone signals for different carrier frequencies of sound (compare corresponding power spectra depicted on the left vertical scale in Fig. 2) and for different integer numbers of lattice constants N as indicated. $N = 0$ corresponds to the reference of no sample. For all carrier frequencies and for $N = 1, 2$, the transmitted pulses are shifted to later times ($\Leftrightarrow \Delta t_N > 0$), i.e., the acoustic wave propagation is slower in the metamaterial compared to air. Furthermore, the signals are strongly attenuated. For $N = 3, 4$, and 5, we do not even detect significant signals that have propagated through the sample (for late times, we find a weak contribution which has propagated through the walls and around the sample). Note that the depicted pulse center frequencies (compare power spectra on the left-hand side of Fig. 2(a)) cover the first band as well as higher bands, for which previously negative refraction (in the sense of a negative angle in Snell's law) has been reported.[4] This means that negative refraction there has a different meaning than negative group velocities of light reported for double-fishnet type metamaterials[5] or as known for decades from the
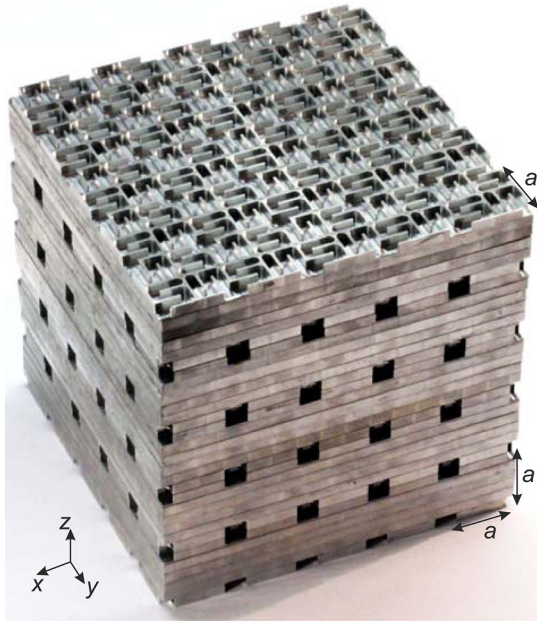
FIG. 3. Photograph of the sample used for the pulse-propagating experiments shown in Fig. 4 composed of $5 \times 5 \times N$ extended unit cells (compare Fig. 1(c)) with variable integer N for $N = 5$.

Garrett and McCumber effect for positive-index materials in the anomalous dispersion regime.[6–8] There,[5–8] the pulse shift on the time axis is opposite, i.e., towards earlier times ($\Delta t < 0$). From the temporal shift Δt_N of the envelope, we can extract the real part of the effective group index $\mathrm{Re}(n)$ via the simple time-of-flight formula $\Delta t_N = (Na)/(c_0/\mathrm{Re}(n)) - (Na)/c_0$. We obtain $\mathrm{Re}(n) = 8 \pm 1.5$, which is consistent with the band-structure calculations shown in Fig. 2. For the first band, this value can also be interpreted as the phase refractive index: Here, the phase that the wave accumulates over one lattice constant a lies in the interval $[-\pi, +\pi]$, equivalent to a shift on the time axis by not more than half a sound period. Consistently, we do not observe major changes of the shape of the transmitted pulse, indicating negligible dispersion. Hence, phase and group velocity of sound are about equal for the first band.

Obviously, some of the higher-order bands in Fig. 2(a) exhibit a negative slope, which does lead to negative refraction at an interface between metamaterial and air like shown previously directly using prism-shaped metamaterial samples.[4] However, as known from solid-state physics or discussed in established photonic crystal textbooks,[9] the phase velocity of these higher bands cannot be defined unambiguously. In one dimension (1D) and for lattice constant a_{1D} ($= a/2$ in our bcc case), this is simple to see: As discussed above, for the first band, the phase change $\varphi = ka_{1D}$ for a wave with wave number $k \in [-\pi/a_{1D}, +\pi/a_{1D}]$ in the first Brillouin zone propagating over one unit cell a_{1D} lies in the interval $[-\pi, +\pi]$. Thus, the phase velocity can uniquely be defined.[10] For the higher-order bands above the first-order Bragg condition, the phase change lies outside of this interval. Due to the lattice periodicity, integer multiples of $\pm 2\pi$ can be added to the phase (or, equivalently, integer multiples of $\pm 2\pi/a_{1D}$ to the wave number). Thus, for example, a phase change of $+1.5\pi$ is strictly equivalent to a phase
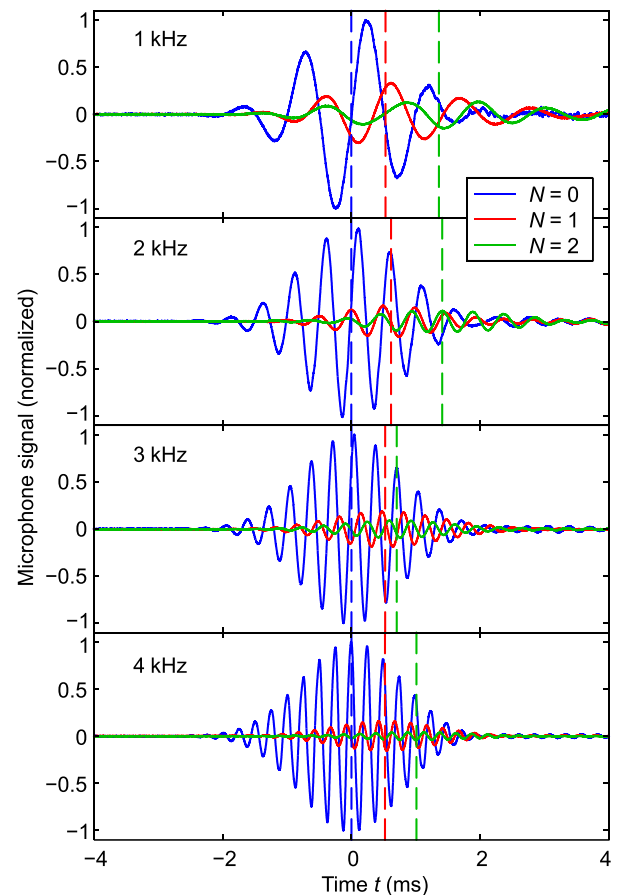

FIG. 4. Measured microphone signals for different carrier frequencies and different integer numbers $N = 0, 1, 2$ of lattice constants a. The extracted peak positions of the pulse envelopes for N = 1, 2 are marked by the vertical dashed lines.

change of -0.5π. The associated modes as well as the transmitted pulses are strictly indistinguishable. One can hence either assign a positive or a negative phase velocity and, equivalently, either a positive or a negative phase refractive index. In other words, one can either look at the wave vector in the reduced zone scheme (i.e., in the first Brillouin zone) or in the extended zone scheme, leading to either positive or negative wave numbers k. This ambiguity means that it is essentially physically meaningless—although not mathematically incorrect—to assign phase velocities or phase refractive indices to these bands. Hence, in contrast to the previous work,[3,4] we refrain from making claims regarding the phase velocity in the higher bands in this Letter. We do emphasize, however, that the propagation results shown in Fig. 4 for frequencies in the higher bands look just the same as those for the first band in that similar shifts are observed. Thus, it is quite natural to speak of positive phase and positive group velocities for the entire frequency range investigated. After all, in optics, a slab of glass would show the same qualitative behavior.

Another aspect that is obvious from inspecting our raw data in Fig. 4 is that the transmitted amplitudes are strongly reduced by the metamaterial. In general, such attenuation can have two different reasons: (i) reflection from the two sample boundaries and (ii) internal losses. (i) At one sample-air interface, the transmitted sound power decreases by factor $(1 - R)$, where the power reflection coefficient obeys

$R = |(Z - Z_0)/(Z + Z_0)|^2$ with the air impedance Z_0 and the metamaterial effective impedance Z. Neglecting multiple reflections (which is justified due to the large damping), transmission through both sample-air interfaces reduces the power by factor $(1 - R)^2$, hence the wave amplitude proportional to the microphone signal by the square root, i.e., by factor $(1 - R)$. (ii) Due to propagation through the effective material over an integer number N of lattice constants a, the wave amplitude decays by factor $\exp(-\mathrm{Im}(k)Na) = \exp(-2\pi/\lambda\,\mathrm{Im}(n)Na)$ with the air wavelength λ. Aspects (i) and (ii) together lead to the ratio of transmitted amplitude after N lattice constants to incident amplitude given by $(1 - R) \times \exp(-2\pi/\lambda\,\mathrm{Im}(n)Na)$. From the comparison with our measured data shown in Fig. 4, we estimate $\mathrm{Im}(n) = 2.0, 0.4, 0.5, 0.8$ and $R = 0.2, 0.8, 0.6, 0.4$ for center frequencies of $1, 2, 3, 4\,\mathrm{kHz}$. This translates into $Z/Z_0 = 3, 15, 8, 5$ and a figure of merit $\mathrm{FOM} \equiv |\mathrm{Re}(n)/\mathrm{Im}(n)| = 5, 25, 13, 11$.[11]

While such FOM still compares favorably with that typical for state-of-the-art optical metamaterials,[11] e.g., for $\mathrm{Im}(n) = 0.5$, it means that the wave amplitude decays from 1 to $\exp(-2\pi \times 0.5) = \exp(-\pi) \approx 1/23$ over a distance of $Na = \lambda$. Hence the acoustic power decays by $23^2 \approx 529$ times over just one air wavelength. This is obviously unacceptable for implementing transformation-acoustics architectures or acoustic focusing lenses but may actually be rather useful for building broadband compact sub-wavelength acoustic absorbers. However, actual applications would require further reducing the reflection by the sample surfaces, i.e., reducing the impedance mismatch to air. Alternative designs for acoustic absorbers have previously been discussed on the basis of lossy sonic crystals.[12–14]

These losses likely arise from a combination of the finite air viscosity (leading to friction at the walls and hence to zero tangential component of the velocity with respect to the wall), from deviations of curl-free velocity fields assumed in the acoustic wave equation, and/or from transfer of heat from the air within the structure channels to the metal walls. One publication[3] on two-dimensional acoustic labyrinthine metamaterials reported $\mathrm{Im}(n) \approx 0.2 - 0.3$, which is on the same order of magnitude as our result. The damping may have been somewhat smaller there because the ratio of surface to inner volume is smaller in two compared to three dimensions. In another publication,[4] the retrieved $\mathrm{Im}(n)$ spectra reveal noise with amplitude of several 0.1 (even negative values corresponding to amplification occur) such that damping on that order might not have been visible within the noise.

In conclusion, we have designed, fabricated, and characterized three-dimensional acoustic labyrinthine metamaterials. We find positive phase and group velocities of sound slower than in air by a factor of about eight over a large range of relevant acoustic frequencies. The losses are very significant though, making these labyrinthine structures an interesting option for sub-wavelength broadband all-angle acoustic absorbers for acoustic-noise suppression. Here, the advantages are that the necessary metamaterial thickness is reduced by the spatial detour in the labyrinth and that the winding channels in the labyrinth with large surface-to-volume ratio lead to enhanced dissipation.

[1]Z. Liang and J. Li, Phys. Rev. Lett. **108**, 114301 (2012).
[2]D. Torrent, A. Håkansson, F. Cervera, and J. Sánchez-Dehesa, Phys. Rev. Lett. **96**, 204302 (2006).
[3]Z. Liang, T. Feng, S. Lok, F. Liu, K. Bo Ng, C. H. Chan, J. Wang, S. Han, S. Lee, and J. Li, Sci. Rep. **3**, 1614 (2013).
[4]Y. Xie, B.-I. Popa, L. Zigoneanu, and S. A. Cummer, Phys. Rev. Lett. **110**, 175501 (2013).
[5]G. Dolling, C. Enkrich, M. Wegener, C. M. Soukoulis, and S. Linden, Science **312**, 892 (2006).
[6]C. G. B. Garrett and D. E. McCumber, Phys. Rev. A **1**, 305 (1970).
[7]A. Puri and J. L. Birman, Phys. Rev. A **27**, 1044 (1983).
[8]S. Chu and S. Wong, Phys. Rev. Lett. **48**, 738 (1982).
[9]J. D. Joannopoulos, S. G. Johnson, J. N. Winn, and R. D. Meade, *Photonic Crystals: Molding the Flow of Light*, 2nd ed. (Princeton University Press, Princeton, 2008).
[10]S. H. Lee, C. M. Park, Y. M. Seo, Z. G. Wang, and C. K. Kim, Phys. Rev. Lett. **104**, 054301 (2010).
[11]C. M. Soukoulis and M. Wegener, Nature Photon. **5**, 523 (2011).
[12]J. Sánchez-Dehesa, V. M. García-Chocano, D. Torrent, F. Cervera, S. Cabrera, and F. Simon, J. Acoust. Soc. Am. **127**, 1777 (2010).
[13]V. M. García-Chocano, S. Cabrera, and J. Sánchez-Dehesa, Appl. Phys. Lett. **101**, 184101 (2012).
[14]V. M. García-Chocano and J. Sánchez-Dehesa, Appl. Acoust. **74**, 58 (2013).